Journal of Materials Chemistry C

Accepted Manuscript

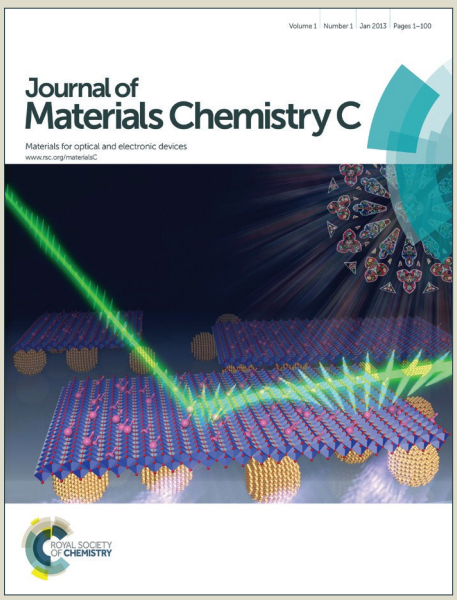

ROYAL SOCIETY OF CHEMISTRY

www.rsc.org/materialsC

Journal of Materials Chemistry C RSCPublishing

ARTICLE

Compatibility of Amorphous Triarylamine Copolymers with Solution-Processed Hole Injecting Metal Oxide Bottom Contacts

Cite this: DOI: 10.1039/x0xx00000x

Stephen Logan,[a] Jenny E. Donaghey,[b] Weimin Zhang,[b] Iain McCulloch[b] and Alasdair J. Campbell[a]*

Received 00th January 2012,
Accepted 00th January 2012

DOI: 10.1039/x0xx00000x

www.rsc.org/

Triarylamine copolymers are p-type organic semiconducting materials which have been shown to have the crucial advantages of being air-stable, forming amorphous films (critical for device uniformity over large areas) and allowing the creation of high mobility transistors and highly efficient perovskite solar cells. A key area of recent technological progress has been the development of solution-processable metal oxides as charge injection layers in organic semiconducting devices. Here we report on the synthesis of a large ionization potential (I_P = 5.65 eV) silafluorene bridged triarylamine copolymer poly(silafluorene-triarylamine) (PSiF-TAA), and compare its time-of-flight (TOF) bulk hole mobility to that of a fluorene bridged triarylamine copolymer poly(fluorene-triarylamine) (PF-TAA), (I_P = 5.4 eV) and the homopolymer polytriarylamine (PTAA) (I_P = 5.2 eV). Using these mobility values and current-voltage measurements, we then quantify the charge injection efficiency (χ) into these polymers from three ambiently-prepared solution processed hole-injecting contacts MoO_3 (aqueous nanoparticle dispersion), V_2O_5 (sol-gel) and chlorinated indium tin oxide (Cl-ITO) (UV - solvent assisted), and compare them to the more conventional contacts ITO and poly(3,4-ethylenedioxythiophene): poly(styrenesulfonate) (PEDOT:PSS). Whilst hole injection into PTAA is relatively unaffected by the nature of the contact, injection into PF-TAA and PSiF-TAA is greatly improved by the use of MoO_3 and Cl-ITO. Despite its similar mobility and larger ionization potential compared to the homopolymer, the highest injection efficiency is achieved for PF-TAA, indicating the role of chemical design in optimizing charge injection into organic semiconductor devices.

Introduction

For the vision of ubiquitous plastic electronics to be realised, it is crucial to develop an understanding of how charge is injected into, and extracted from, conjugated polymer organic semiconductors. The charge injection efficiency (χ) is a critical parameter that can determine the performance and efficiency of organic semiconducting devices including organic light emitting diodes (OLEDs), organic thin-film-transistors (OTFTs) and organic photovoltaics (OPVs).[1–3] Polymers are an important class of organic semiconductor because of their inherent properties of being solution processable, lightweight, flexible and amenable to a range of scalable, high throughput manufacturing methods such as roll-to-roll printing[4]. Triarylamine copolymers have previously been investigated as p-type OTFT materials and have been shown to have the crucial advantages of being air-stable, forming amorphous films (critical for device uniformity over large areas) and having hole mobility values as high as 10^{-2} cm^2/Vs.[5] Poly(triarylamine) (PTAA) and poly(fluorene-co-triarylamine) (PF-TAA) have been used in small molecule-polymer blends in solution procesed OTFTs to help the small molecule yield field effect mobilities in excess of 5 cm^2/Vs, making them attractive for use in commercial applications.[6] More recently the use of PTAA as a hole transporting material (HTM) in perovskite solar cells has lead to significant performance gains with recorded device efficiencies of over 16%.[7,8] PF-TAA has been investigated as a HTM in perovskite solar cells[9] and as a light emitting polymer has also been used as the active layer in solution processed OLEDs.[10,11]

However, fluorene bridged trairylamines and other state-of-the-art-polymers can have large ionisation potentials (>5.4eV), which makes it difficult to inject holes from the commonly used contacts such as gold (workfunction ~5.1eV) in OTFTs and Indium Tin Oxide (ITO) (workfunction ~4.8eV) in OLEDs and OPVs due to the

presence of a potential barrier. Poly(3,4-ethylenedioxythiophene): poly(styrenesulfonate) (PEDOT:PSS), a conducting polymer, is commonly used as a hole injection/extraction layer in OLEDs and OPVs or as the source-drain contacts in OTFTs. However, its work-function is still relatively low (5.2eV) and it has been associated with reduced device lifetimes through chemical degradation of organic layers due to its acidic and hygroscopic nature.[12]

Therefore, research continues in an endeavour to find alternative hole injecting materials and/or surface treatments that can enhance organic semiconductor device performance. One approach has been the thermal evaporation of high workfunction transition metal oxide (TMO) materials including molybdenum trioxide (MoO_3), vanadium pentoxide (V_2O_5) and tungsten oxide (WO_X) as contacts to create hybrid (Inorganic-Organic) devices.[13–16] These transition-metal oxides have been shown to be very effective at forming hole injecting contacts with organic semiconductors with ionisation potentials as high as 6.2eV and have been used in OLEDs, OPVs and OTFTs.[17] It is considered highly desirable to solution process the metal oxide material in ambient conditions to ensure compatability with high throughput printing methods of manufacture. However, processing from solution and/or exposing the metal oxide to air has been shown to significantly alter its energetic structure and typically lowers the workfunction, making the potential effectiveness of such approaches uncertain.[18,19]

Ambient solution processing methods for TMOs have recently been reported for MoO_3 (via aqueous nanoparticle dispersion) and V_2O_5 (via a sol-gel method) in OPV devices and have shown comparable performance to those using PEDOT:PSS.[20,21] OLED devices with record efficiencies have also been demonstrated using a UV light - solvent assisted process to engineer a single atomic layer of chlorine onto the surface of ITO to create chlorinated ITO (Cl-ITO) contacts with a workfunction of 6.1eV.[22] Polymer OLEDs with solution processed ZnO and V_2O_5 injection layers show equal performance to conventional contact devices but with improved stability.[23] Polymer OTFTs with solution processed MoO_3 on the Au source and drain contacts showed reduced contact resistance and a higher mobility.[24] A clear methodology to quantify the injection efficiency of such contacts will greatly improve our understanding of the comparative performance of such materials. Additionally, by investigating charge injection into amorphous triarylamine copolymers, the complication of variations in crystallinity can be avoided, allowing clearer identification of the role of chemical structure, and how chemical design can be used to optimise hole injection.

Results and Discussion

Here we report on charge transport time of flight (TOF) bulk hole mobility measurements of the p-type polymer polytriarylamine PTAA (ionization potential (I_P) = 5.2 eV), its fluorene copolymer PF-TAA (I_P = 5.4 eV),[5] and a novel silafluorene bridged triarylamine copolymer poly(silafluorene-triarylamine) (PSiF-TAA) (I_P = 5.65 eV) (see **Figure 1d**) (see Supplementary Information for PSiF-TAA synthesis). For each of these three polymers we use current-density - voltage space charge limited current analysis to quantify the injection efficiency (χ) of ambiently-prepared solution processed hole-injecting contacts including MoO_3 (aqueous nanoparticle dispersion), V_2O_5 (sol-gel) and Cl-ITO (UV - solvent assisted). These are then assessed with reference to devices using conventional contacts ITO and PEDOT:PSS.

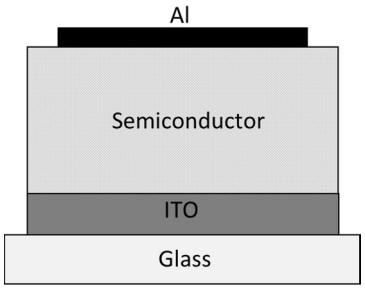

(a)

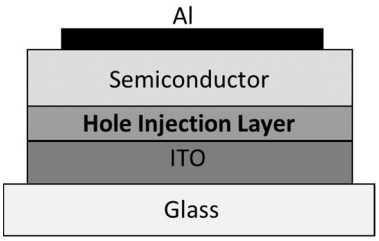

(b)

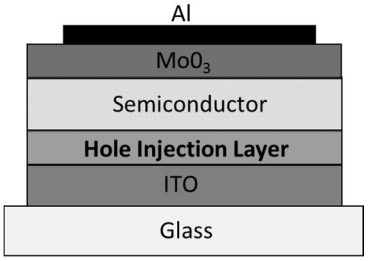

(c)

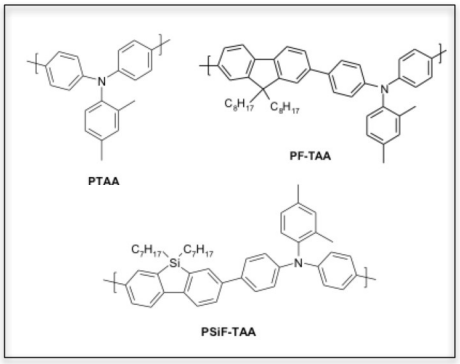

(d)

Figure 1. (a) Device structure for TOF measurements used for all three polymers**.** (b) Device structure for J-V measurements with PTAA. (c) Device structure for J-V measurements with PF-TAA and PSiF-TAA. (d) Chemical structure of PTAA, PF-TAA and PSiF-TAA

PTAA, PF-TAA and PSiF-TAA devices for TOF measurements were fabricated with an ITO/polymer/Al architecture (**Figure 1a**) and a polymer film thickness of 0.9-2.3 μm. A sheet of holes were photogenerated underneath the positively biased ITO contact using a pulse from a 355nm Nd:Yag laser, and traversed the semiconducting polymer layer to yield current vs. time plots as shown in **Figure 2a**, **b** and **c**. TOF transients were measured for a range of different electric fields for each polymer at room temperature, and the hole mobility calculated using the equation[25]:

$$\mu = \frac{d^2}{t_{tr}(V - V_{bi})} \qquad (1)$$

where μ is the charge carrier mobility, d is the thickness of the semiconductor layer, t_{tr} is the transit time (here taken at the transient inflexion point), V is the applied voltage and V_{bi} is the built-in voltage. The field dependence of the hole mobility is shown in **Figure 2d**, where the applied electric field $E = (V-V_{bi})/d$.

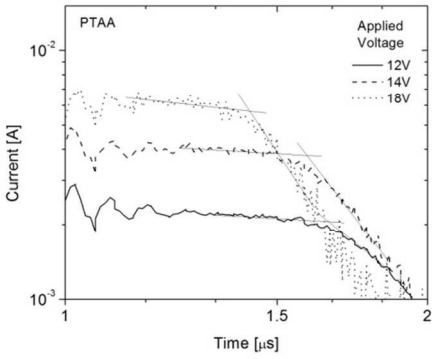

(a)

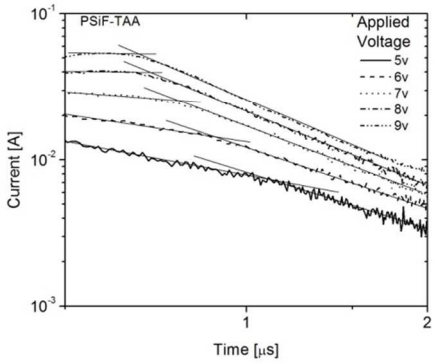

(b)

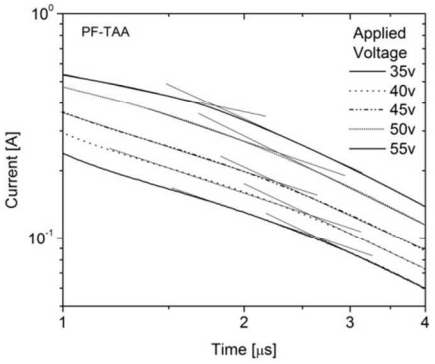

(c)

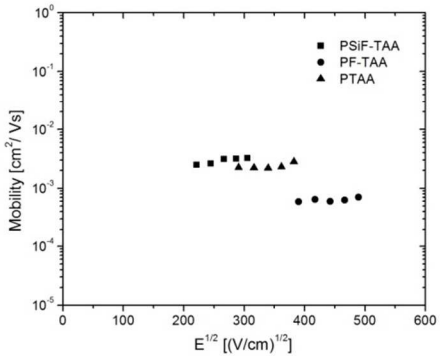

(d)

Figure 2. Representative TOF transients for (a) PTAA (d = 1.3 μm), (b) PF-TAA (d = 2.4 μm) and (c) PSiF-TAA (d = 0.9 μm) with marked transit times at various electric fields. (d) Field dependence of mobility for PTAA, PF-TAA and PSiF-TAA

For PTAA, transport was non-dispersive, which is consistent with previous TOF results.[26] For PF-TAA and PSiF-TAA transport was instead dispersive, indicating more energetic disorder in the transport density of states (DOS) or the presence of additional deep traps. Despite this and the differences in chemical structure and ionization potential, the magnitude and field dependence of the bulk hole mobility for this film thickness range are similar for PTAA, PF-TAA and PSiF-TAA, being $1.1x10^{-3}$ cm^2/Vs (at $E = 1x10^5$ V/cm), $0.65x10^{-3}$ cm^2/Vs (at $2x10^5$ V/cm), and $3.1x10^{-3}$ cm^2/Vs (at $0.7x10^5$ V/cm) respectively. This suggests that the triarylamine units dominate interchain transport, and that hopping distances and overlap integrals are very similar. However the sifluorene polymer has a higher hole mobility than the fluorene polymer. The reason for the enhanced mobility is not entirely clear. It is known that differences in molecular weight can have a significant affect on charge transport in conjugated systems and the molecular weight of PF-TAA (Mn 28, Mw 53) is lower than that of PSiF-TAA (Mn 29, Mw 75). Current-density voltage (JV) measurements were then used to systematically study charge injection into PTAA, PF-TAA and PSiF-TAA. A range of solution processed hole-injecting contacts

were investigated including molybdenum trioxide nanoparticles (MoO_3), vanadium pentoxide prepared using a sol-gel method (V_2O_5), and chlorinated ITO (Cl-ITO), which have estimated/measured workfunctions of 5.3 eV,[20] 5.3-5.6 eV,[21] and 6.1eV[22] respectively. These were then compared with reference devices using the conventional contacts plasma-cleaned ITO and PEDOT:PSS, which have measured workfunctions of 5.1 eV and 5.2 eV respectively.[27,28]

Hole only diodes were fabricated for PTAA with the structure shown in **Figure 1b.** It was found that for PF-TAA and PSiF-TAA, an additional MoO_3 top layer was required to prevent electron injection from the Al contact and ensure hole only devices (**Figure 1c**). The results from the JV measurements are shown in **Figure 3** with current-density J plotted against drive bias minus the built-in potential ($V-V_{bi}$) (see Supplementary Information for original JV data).

The built-in potential was measured using the photocurrent technique (see Supplementary Information). For PTAA, PF-TAA and PSif-TAA, V_{bi} does not vary with the injecting contact, indicating Fermi level pinning at the polymer/contact interface. The respective V_{bi} values of ~ +1V, ~ -0.4V and ~ 0V are consistent with pinning to the polymer highest occupied molecular orbital (HOMO) levels given Al and MoO_3/Al top contact workfunctions of respectively 4.2eV and 5.7-5.8eV. Such pinning has previously been observed by small molecules evaporated on metal oxides[29], and the results shown here also suggest that the same effect occurs with PEDOT:PSS, consistent with early experimental evidence.[30,31] This points towards something quite fundamental between the alignment of the contact Fermi levels and the HOMO levels in such material systems.

The trap-free space charge limited current (TFSCLC) J_{TFSCLC} is the maximum current possible for a single-carrier organic semiconductor device and requires an ideal Ohmic contact with an injection efficiency value of 1. The TFSCLC, accounting for the field dependence of the mobility, is given by the Murgatroyd equation[32]:

$$J_{TFSCLC} = \frac{9}{8}\varepsilon_r\varepsilon_0\mu\frac{(V-V_{bi})^2}{d^3}e^{0.89\gamma\sqrt{\frac{V-V_{bi}}{d}}} \qquad (2)$$

where ε_0 is the absolute permittivity, ε_r is the polymer dielectric constant ($\varepsilon_r = 3$), μ_0 is the zero-field mobility, and γ is a measure of the field dependence of the mobility. Values of μ_0 and γ can be found by fitting the TOF hole mobility□μ in **Figure 2d** to[33]:

$$\mu = \mu_0 e^{\gamma\sqrt{\frac{V-V_{bi}}{d}}} \qquad (3)$$

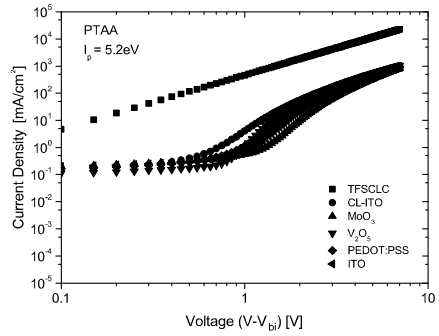

(a)

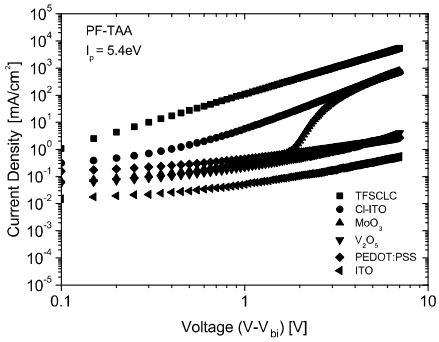

(b)

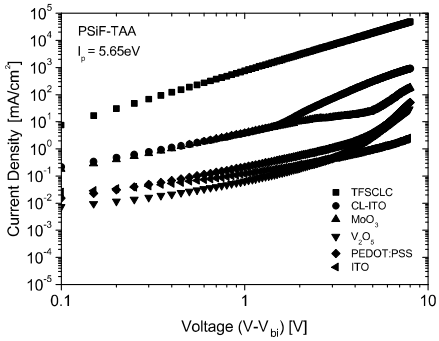

(c)

Figure 3. Graphs showing JV curves for injecting contacts Cl-ITO, MoO_3, V_2O_5, PEDOT:PSS, ITO (oxygen plasma treated) and the ideal TFSCLC for (a) PTAA, (b) PF-TAA and (c) PSiF-TAA.

J_{TFSCLC} is plotted against ($V-V_{bi}$) in **Figure 3**. Injection efficiency χ is an absolute measure of the efficiency of an injecting contact (for a given value of d and E)[34]:

$$\chi = \frac{J_{measured}}{J_{TFSCLC}} \qquad (4)$$

where $J_{measured}$ is the measured current. Values of χ at E = $5x10^5$ V/cm ($(V-V_{bi})$ ~6V) for all devices are shown in **Figure 4**. (We note that the dispersive nature of hole transport in PF-TAA and PSiF-TAA means that the non-dispersive equilibrium mobility values will be slightly lower than shown in Figure 2d. Hence, for these two copolymers, the values of χ in Figure 4 must be taken as lower limits of the actual equilibrium injection efficiency).

The J vs $(V-V_{bi})$ characteristics (**Figure 3**) for all contacts and polymers show similar features. At low $(V-V_{bi})$ bias values the characteristics follow a slope of about 1 for injection-limited or ohmic conduction.[35] The current then undergoes a rapid increase with a slope > 2 which can be associated with the filling of traps distributed in energy at the contact/polymer interface.[36] Above the trap-free limit, the characteristics run parallel to J_{TFSCLC}, indicating TFSCLC with $\chi < 1$, the χ value associated with the barrier-pinned quasi-ohmic contact combined with the effect of any further shallow interfacial traps due to reduced injection pathways from poor polymer interfacial packing.[37,38] Values of χ (**Figure 4**) in the TFSLC regime for PTAA, PF-TAA and PSiF-TAA are in the range previously reported for polyphenylenevinylene and polyfluorene copolymers.[38]

For PTAA (**Figure 3a**), the magnitude of the current in the low bias injection-limited/ohmic regime is similar for all devices. The bias value of the onset of the trap-filling regime does vary, being lower for the larger workfunction contacts. Above the trap-free limit at high bias, the current is also similar for all devices. All contacts show similar values of injection efficiency (**Figure 4a**).

PTAA has a low ionization potential of 5.2 eV, so for the contacts used here with workfunctions ranging from 5.1 to 6.1 eV, we might expect the injection barrier to be pinned to about the same level. This would explain the similarity in the JV characteristics for the different contacts. The value of χ is low for all the contacts, being between 0.03 and 0.05 and showing little variation. The magnitude is surprising given that the low PTAA ionization potential should minimize the pinned injection barrier. However, metal oxides have been shown to pin the conduction band/HOMO injection barrier to values ≥ 0.3 eV, so we may be in the barrier-pinned quasi-ohmic contact regime. The lack of variation in χ is also surprising given the physical differences of the contact surfaces, being both organic and inorganic and likely to vary considerably in nanoscale surface roughness; we might expect a variation in the injection pathways depending on how the polymer chains pack on the different surfaces, but this appears to be remarkably uniform.

Thus, although PTAA gives very uniform behaviour with different bottom contacts, overall hole injection into the homopolymer is surprisingly low, and may lead to contact resistance effects in devices.

For PF-TAA (**Figure 3b**), the magnitude of the current in the low bias injection-limited/ohmic regime varies, being lowest for ITO and highest for Cl-ITO. The onset of the trap-filling regime is never achieved for the lower workfunction contacts ITO, PEDOT;PSS and V_2O_5. For MoO_3 the onset is higher than for PTAA. For the Cl-ITO devices, the change in magnitude and gradient from the low to high bias regimes is minimal, indicative of a remarkably trap free interface. For PF-TAA, only the MoO_3 and Cl-ITO devices achieve TFSCLC with $\chi < 1$.

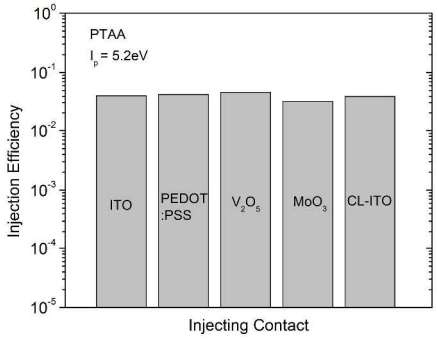

(a)

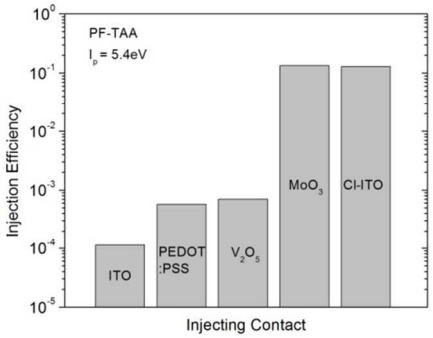

(b)

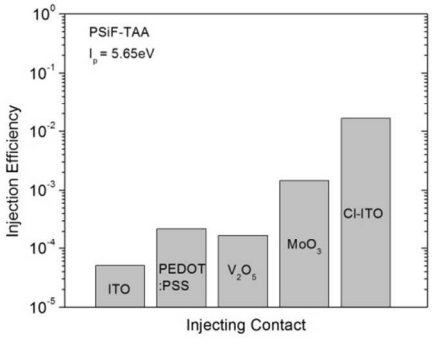

(c)

Figure 4. Bar charts showing the measured hole injection efficiencies of the five injecting contacts for (a) PTAA, (b) PF-TAA and (c) PSiF-TAA in ~100nm films at field $5x10^5$ V/cm.

The injection efficiency values (**Figure 4b**) for the ITO, PEDOT;PSS and V_2O_5 devices are all < 0.001, decreasing with decreasing contact workfunction. This, and the lack of a TFSCLC regime, is indicative of barrier-limited injection into PF-TAA (I_P = 5.4 eV) for these low workfunction contacts. The Cl-ITO and MoO_3 devices, however, have $\chi > 0.1$. These are high values, and indicative of low injection barriers combined with multiple injection pathways due to optimum polymer chain packing on the contact surfaces.

PF-TAA also has a field-effect mobility μ_{FET} an order of magnitude higher than the bulk mobility measured here, whilst for PTAA the values are approximately equal.[5] This would be consistent with PF-TAA having enhanced packing at interfaces compared to the homopolymer PTAA.

For PSiF-TAA (**Figure 3c**), the magnitude of the current in the low bias injection-limited/ohmic regime roughly decreases with decreasing contact workfunction. The onset of the trap-filling regime is never achieved for ITO, but for the other contacts it is shifted to higher biases than for PTAA. Only the Cl-ITO devices achieve TFSCLC with $\chi < 1$.

The χ values (**Figure 4c**) for the ITO, PEDOT;PSS and V_2O_5 devices are all < 0.001, and lie below the values for PF-TAA. This is consistent with barrier-limited injection and the deeper HOMO level of PSiF-TAA (I_P = 5.65 eV). The appearance of the onset of the trap-filling regime for PEDOT;PSS and V_2O_5 suggests that there are more traps at the interface for these contacts than for PF-TAA, where this regime is not observed. The inability to achieve the TFSCLC regime for the MoO_3 contact in comparison to PF-TAA can be explained in terms of the difference in I_P resulting in a larger injection barrier. The fact that only the Cl-ITO devices reach TFSCLC confirms that large workfunction contacts are required to optimise injection into a polymer with an ionization potential of order 5.65 eV.

As TFSCLC was achieved for all three polymers with Cl-ITO, we can compare the injection efficiency values. These are 0.04, 0.14 and 0.02 (d = 100 nm, F = $5x10^5$ V/cm) for PTAA, PF-TAA and PSiF-TAA, respectively. Thus the fluorene copolymer can achieve the best charge injection when compared to the homopolymer and the silafluorene copolymer, the latter two having remarkably similar properties when matched with a large workfunction contact.

Finally, in terms of the TMO contacts themselves, V_2O_5 appears to give very similar injection behaviour to PEDOT:PSS for all three polymers. The MoO_3 nanoparticles also perform better than the sol-gel V_2O_5, despite its apparently similar workfunction. However, for a large I_P polymer, only CL-ITO can act as an ohmic contact, indicating the necessity of developing such large workfunction contacts.

Conclusions

Bulk hole transport has been measured for the first time in bridged triarylamine copolymers PF-TAA and novel PSiF-TAA and compared with homopolymer PTAA. Average bulk mobility values were observed to be similar and have a low field dependence. The fluorene and silafluorene copolymer transients however showed dispersive transport properties, indicating a higher degree of energetic disorder compared to the homopolymer. The mobility of the polymers can be attributed to various factors, in particular the morphology and molecular weight, neither of which is dependent on ionisation potential. The ionisation potential is a function of the electron density of the conjugated system and the electron donating nitrogen atoms in PTAA help to lower the ionisation potential. The injection efficiency measurements support the reported ionisation potential values for all three polymers and workfunction values for the injecting contacts with a consistent relationship between workfunctions, HOMO levels and device currents. PF-TAA also achieves the best hole injection efficiency values of the three polymers, showing how the influence of chemical structure can override such factors as ionization potential. One possible explanation for this may be a higher degree of energetic disorder in the PF-TAA (supported by its highly dispersive transport characteristics) relative to the other polymers that may allow for charge to be injected into the tail states of the density of states, effectively lowering the barrier height.

For each of these polymers, the hole injection JV characteristics and injection efficiency of ambient, solution processed MoO_3 nanoparticle, sol-gel V_2O_5 and Cl-ITO contacts were then measured and compared with common anode materials ITO and PEDOT:PSS. The injection efficiency of V_2O_5 is comparable with that of PEDOT:PSS, so it may be a suitable substitute in OPV and OLED applications. However, for materials with larger ionization potentials, MoO_3 or Cl-ITO are better injecting contacts, with Cl-ITO giving the best overall performance.

Experimental Methods

All bottom contacts were processed in a cleanroom environment under ambient conditions. ITO on glass substrates (Psiotec 15Ω/□) were subjected to a standard cleaning protocol via sonication in detergent, acetone and isopropanol followed by O_2 plasma treatment. ITO devices were used as prepared. PEDOT:PSS (Clevios P, HC Stark) was spincoated at 3000 rpm for 1 minute and baked at 150°C for 20 minutes to give a film thickness of 50nm. V_2O_5 sol-gel was prepared according to [17] via mixing oxytrisopropoxide in isoporopanol 1:70 ratio, then spincoated at 8000rpm for 1 minute to give a film of thickness 15nm and left in air to hydrolyse for 1 hour. MoO_3 nanoparticle dispersion was prepared according to [16] from an ammonium molybdate precursor solution and then spin-coated at 3000rpm for 3 minutes to produce a surface covering of nanoparticles. Cl-ITO was prepared according to method given by [18] where ITO substrates were UV exposed in a sealed reaction vessel containing 1,2-dichlorobenzene (99.99% Sigma Aldrich) and O_2 plasma treated for 10 minutes (Emitech 1050X). PTAA, PF-TAA were synthesized as given by [5]. For PSiF-TAA synthesis see Supporting Information. Polymer solutions of various concentrations (20-100mg/ml) in chlorobenzene (99.99% Sigma Aldrich) were spin-coated at different speeds to give film thicknesses ~100nm for JV and 0.9-2.3μm for TOF (Dektak 3 Alphastep). All polymer films were annealed for 20 minutes at 110°C and transferred to nitrogen filled glovebox for top contacts deposition. 10nm of MoO_3 (99.99% Sigma Aldrich) was deposited via shadow mask under vacuum at pressure $5.5x10^{-6}$ mBar. The 100 nm Al top contacts were deposited under the same conditions. Average device area was 0.045 cm^2. Devices were measured under vacuum immediately after preparation. A frequency tripled Quantel Nd:YAG laser (excitation wavelength 355nm), a Tektronix 3052 oscilloscope and a bespoke

voltage source was used for TOF. JV measurements were taken using a Keithley 2400 Source Measure Unit.

Acknowledgements

The authors thank the UK EPSRC for funding Stephen Logan at the Plastic Electronics Doctoral Training Centre (grant EP/G037515/1).

Notes and references

[a] Stephen Logan, Dr. Alasdair J. Campbell,
Department of Physics and the Centre for Plastic Electronics,
Imperial College London, South Kensington campus, London, SW7 2AZ (United Kingdom)
E-mail: stephen.logan09@imperial.ac.uk; alasdair.campbell@imperial.ac.uk

[b] Jenny E. Donaghey, [+]Dr. Weimin Zhang, Prof. Iain McCulloch,
Department of Chemistry and the Centre for Plastic Electronics,
Imperial College London, South Kensington campus, London, SW7 2AZ (United Kingdom)

[+] Second address: Guangxi University for Nationalities, Nanning 530006, P.R. China

Electronic Supplementary Information (ESI) available: Details of the synthesis of PSiF-TAA, JV characteristics, photocurrent and built-in-voltage measurements. See DOI: 10.1039/b000000x/

1. H. Bässler, *Phys. status solidi*, 1993, **175**, 15–56.
2. Y. Shirota and H. Kageyama, *Chem. Rev.*, 2007, **107**, 953–1010.
3. A. J. Campbell, D. D. C. Bradley and H. Antoniadis, *Appl. Phys. Lett.*, 2001, **79**, 2133.
4. S. R. Forrest, *Nature*, 2004, **428**, 911–918.
5. W. Zhang, J. Smith, R. Hamilton, M. Heeney, J. Kirkpatrick, K. Song, S. E. Watkins, T. Anthopoulos and I. McCulloch, *J. Am. Chem. Soc.*, 2009, **131**, 10814–5.
6. J. Smith, W. Zhang, R. Sougrat, K. Zhao, R. Li, D. Cha, A. Amassian, M. Heeney, I. McCulloch and T. D. Anthopoulos, *Adv. Mater.*, 2012, **24**, 2441–2446.
7. J. H. Heo, S. H. Im, J. H. Noh, T. N. Mandal, C.-S. Lim, J. A. Chang, Y. H. Lee, H. Kim, A. Sarkar, M. K. Nazeeruddin and others, *Nat. Photonics*, 2013, **7**, 486–491.
8. N. J. Jeon, J. H. Noh, Y. C. Kim, W. S. Yang, S. Ryu and S. Il Seok, *Nat. Mater.*, 2014.
9. S. Ryu, J. H. Noh, N. J. Jeon, Y. C. Kim, W. S. Yang, J. W. Seo and S. Il Seok, *Energy Environ. Sci.*, 2014.
10. S. L. M. Van Mensfoort, M. Carvelli, M. Megens, D. Wehenkel, M. Bartyzel, H. Greiner, R. A. J. Janssen and R. Coehoorn, *Nat. Photonics*, 2010, **4**, 329–335.
11. M. Carvelli, R. A. J. Janssen and R. Coehoorn, *Phys. Rev. B*, 2011, **83**, 75203.
12. F. So and D. Kondakov, *Adv. Mater.*, 2010, **22**, 3762–77.
13. H. Schmidt, H. Flügge, T. Winkler, T. Bülow, T. Riedl and W. Kowalsky, *Appl. Phys. Lett.*, 2009, **94**, 243302.
14. J. Meyer, K. Zilberberg, T. Riedl and A. Kahn, *J. Appl. Phys.*, 2011, **110**, 33710.
15. J. Meyer, T. Winkler, S. Hamwi, S. Schmale, H.-H. Johannes, T. Weimann, P. Hinze, W. Kowalsky and T. Riedl, *Adv. Mater.*, 2008, **20**, 3839–3843.
16. L. P. Lu, C. E. Finlayson and R. H. Friend, *Semicond. Sci. Technol.*, 2014, **29**, 25005.
17. J. Meyer, S. Hamwi, M. Kröger, W. Kowalsky, T. Riedl and A. Kahn, *Adv. Mater.*, 2012, **24**, 5408–27.
18. H. Ding, Y. Gao, C. Small, D. Y. Kim, J. Subbiah and F. So, *Appl. Phys. Lett.*, 2010, **96**, 243307.
19. M. C. Gwinner, R. Di Pietro, Y. Vaynzof, K. J. Greenberg, P. K. H. Ho, R. H. Friend and H. Sirringhaus, *Adv. Funct. Mater.*, 2011, **21**, 1432–1441.
20. F. Liu, S. Shao, X. Guo, Y. Zhao and Z. Xie, *Sol. Energy Mater. Sol. Cells*, 2010, **94**, 842–845.
21. K. Zilberberg, S. Trost, H. Schmidt and T. Riedl, *Adv. Energy Mater.*, 2011, **1**, 377–381.
22. M. G. Helander, Z. B. Wang, J. Qiu, M. T. Greiner, D. P. Puzzo, Z. W. Liu and Z. H. Lu, *Science*, 2011, **332**, 944–7.
23. P. de Bruyn, D. J. D. Moet and P. W. M. Blom, *Org. Electron.*, 2012, **13**, 1023–1030.
24. D. Kumaki, Y. Fujisaki and S. Tokito, *Org. Electron.*, 2013, **14**, 475–478.
25. D. Hertel and H. Bässler, *Chemphyschem*, 2008, **9**, 666–88.
26. S. Barard, M. Heeney, L. Chen, M. Cölle, M. Shkunov, I. McCulloch, N. Stingelin, M. Philips and T. Kreouzis, *J. Appl. Phys.*, 2009, **105**, 013701.
27. H. Y. Yu, X. D. Feng, D. Grozea, Z. H. Lu, R. N. S. Sodhi, a-M. Hor and H. Aziz, *Appl. Phys. Lett.*, 2001, **78**, 2595.
28. V. Shrotriya, G. Li, Y. Yao, C.-W. Chu and Y. Yang, *Appl. Phys. Lett.*, 2006, **88**, 073508.
29. M. T. Greiner, M. G. Helander, W.-M. Tang, Z.-B. Wang, J. Qiu and Z.-H. Lu, *Nat. Mater.*, 2012, **11**, 76–81.
30. C. Tengstedt, W. Osikowicz, W. R. Salaneck, I. D. Parker, C.-H. Hsu and M. Fahlman, *Appl. Phys. Lett.*, 2006, **88**, 053502.
31. H. Peisert, A. Petr, L. Dunsch, T. Chassé and M. Knupfer, *ChemPhysChem*, 2007, **8**, 386–390.
32. M. A. Lampert and P. Mark, 1970.

33. S. V Novikov, D. H. Dunlap, V. M. Kenkre, P. E. Parris and A. V Vannikov, *Phys. Rev. Lett.*, 1998, **81**, 4472.

34. M. Abkowitz, J. S. Facci and J. Rehm, *J. Appl. Phys.*, 1998, **83**, 2670–2676.

35. S. C. Jain, W. Geens, a. Mehra, V. Kumar, T. Aernouts, J. Poortmans, R. Mertens and M. Willander, *J. Appl. Phys.*, 2001, **89**, 3804.

36. H. Bässler and A. Köhler, *Top. Curr. Chem.*, 2012, **312**, 1–65.

37. L. G. Kaake, P. F. Barbara and X.-Y. Zhu, *J. Phys. Chem. Lett.*, 2010, **1**, 628–635.

38. M. J. Harding, D. Poplavskyy, V.-E. Choong, F. So and A. J. Campbell, *Adv. Funct. Mater.*, 2010, **20**, 119–130.

